



Deposited via The University of Leeds.

White Rose Research Online URL for this paper:

<https://eprints.whiterose.ac.uk/id/eprint/145122/>

Version: Accepted Version

Article:

York, DW, Collins, S and Rantape, M (2019) Measuring the permeability of thin solid layers of natural waxes. *Journal of Colloid and Interface Science*, 551. pp. 270-282. ISSN: 0001-8686

<https://doi.org/10.1016/j.jcis.2019.03.104>

© 2019 Published by Elsevier Inc. Licensed under the Creative Commons Attribution-Non Commercial No Derivatives 4.0 International License (<https://creativecommons.org/licenses/by-nc-nd/4.0/>).

Reuse

This article is distributed under the terms of the Creative Commons Attribution-NonCommercial-NoDerivs (CC BY-NC-ND) licence. This licence only allows you to download this work and share it with others as long as you credit the authors, but you can't change the article in any way or use it commercially. More information and the full terms of the licence here: <https://creativecommons.org/licenses/>

Takedown

If you consider content in White Rose Research Online to be in breach of UK law, please notify us by emailing eprints@whiterose.ac.uk including the URL of the record and the reason for the withdrawal request.

Title name: Measuring the permeability of thin solid layers of natural waxes

Authors: David W. York, Stephen Collins and Mooketsi Rantape

Address: School of Chemical and Process Engineering, University of Leeds, Leeds LS2 9JT, UK

Corresponding author:

Dr Stephen Collins,
School of Chemical and Processing Engineering
University of Leeds
Leeds LS29JT
UK
Telephone: +44 113 343 6172
Email: mtlsc@leeds.ac.uk

Email addresses:

David York	D.W.York@leeds.ac.uk
Stephen Collins	mtlsc@leeds.ac.uk
Mooketsi Rantape	mocksruf@yahoo.com

Abstract

Hypothesis

Previous experimental work has shown that microcapsule walls, made by solidification of a molten wax, are unexpectedly permeable. The hypothesis was that this was due more to the structure of the wall than the material itself.

Experiments

The permeability of thin (sub and low micron thickness) natural waxes was measured where a membrane was placed between two cells and the diffusion of a dye (fluorescein) measured. A filter paper was used to support the membranes. Two methods were used to coat the filter paper; simple dipping and spin coating. The resulting surfaces were examined using SEM, XRD and contact angle.

Findings

Results indicate that the permeability of very thin walled capsules can be investigated by forming a layer on a porous support and measuring diffusion rates. Both the composition of the wax and the sample preparation is extremely important to the structure and resulting permeability of the membranes. Spin coating was much more effective than dip coating in reducing permeability. Carnauba wax had a much lower permeability than beeswax.

A difference in levels between the two cells was observed, indicating a potential Osmotic pressure difference at play which should be further investigated.

Key words: diffusion, permeability, micro encapsulation, food additives, beeswax, carnauba wax

1. Introduction

Much interest has been shown in coating foods and food additives using hydrophobic coatings for protection to limit penetration of water and oxygen from outside as well as loss of internal components such as flavours or migration within a food [1-6].

The coating of food ingredients has been achieved by a range of different materials, including proteins, carbohydrates, lipids, fats and gums [1]. Natural waxes would seem to be suitable for micro encapsulation for aroma components since they are solid at ambient temperatures, can provide superior handling, especially if the aroma ingredients are liquid oils, by converting them into solid particles that are stable, inert and free flowing and are considered safe. They provide a long term retention of compounds not only with high partition coefficients (o/w) for lipophilic compounds, but also with low ones [7]. The relatively low cost and ease of handling of natural waxes has been used to provide melt coating for relatively large, easy to handle confectionary products such as Jelly Beans.

Natural waxes, such as beeswax and plant waxes (e.g. candelilla and carnauba) are available in food grade quality and are permitted in the European Union (E901-903). They exhibit interesting rheology and micro structure. At room temperature wax is ductile without cracking [2,8]. There are indications that in waxes plate like crystals are formed which are more efficient in hampering diffusion of small molecules (i.e. low molecular weight) compounds [2,8,9].

Carnauba wax is produced by the leaves of the carnauba palm *Copernicia prunicia* [10] and is the hardest, highest melting (90°C) natural commercial wax [9]. Compared to other waxes (such as beeswax), carnauba wax is significantly less viscous (and hence easier to manipulate during processing), more elastic and more resistant to deformations [11] eg on resistance to penetration with a 60° cone at 3mm penetration, ~32N was required for beeswax and ~246 N for carnauba wax [11].

Waxes are also amenable to a wide range of standard processing techniques such as spray drying, congealing fluid bed spray coating, spray chilling or melt injection and have been applied to flavour ingredients such as ethyl vanillin [1,9]. Their relatively low melting temperature is also an advantage to coating/encapsulation in that thermally sensitive materials (such as those with high volatility) can be processed with low losses.

However, despite the ease of handling (melting point and viscosity) very limited work has been published in the use of natural waxes for micro encapsulation especially their permeability. Micro encapsulation has advantages for stability, controlled release and being able to be non-detectable by consumers due to their size.

A particularly useful route to forming micro encapsulates has been that of Collins *et al* [12] whereby an aqueous active component is emulsified in molten wax, which is then turned into a double emulsion and the resulting product cooled to induce solidification of the wax to form a solid micro encapsulate with narrow size distribution in the 1 to 100 micron range. The resulting wall thickness is then in the nano to low micron size range eg 17µm capsules had wall thickness of ~2µm [12]. Experimental results from this work indicated a much higher permeability than would have been expected, based on the hydrophobic nature of the wall material. This thin wall will be more dependent on how its structure develops by melt crystallisation during cooling than the much thicker walls that are typical of spray coating processes. or other, more typical ways of making a solid wall for micro encapsulates; such as interfacial reactions or polymer deposition. The protective properties of such a core shell encapsulate will be very dependent on the inherent permeability of the active species in the

wax wall material as well as the micro structure that the wax forms as it solidifies. To date this property of a wax wall has not been studied. Calculating the permeability of the wax walls from experiments involving micro capsules would be highly unreliable since there is a wide distribution of particles size, and no evidence of how wall thickness varied, all of which would impact on rate of release. Consequently, this work was carried out to seek possible explanations for such high permeability in order that future work could produce much more stable encapsulates. Therefore, a means of experimentally studying this permeability, especially the structure of the solid wax was undertaken, using a flat surface for ease of characterisation, as well as studying its dependence on wall chemistry and how the solid structure is formed has been the subject of this paper. One problem was that the mechanical properties of such a thin, wax wall was not strong enough to support the wax, and so a porous support structure was used.

2. Experimental

2.1 Materials

Chemicals used were fluorescein sodium salt (CAS-No. 518-47-8, Sigma Aldrich) which is a dark red powder with molecular weight 376.3g/mole, and has a Stokes–Einstein radius of 0.45 nm [13]; deionised water (Elix Millipore), hydrophilic Durapore® membranes (PVDF, Millipore) 25mm, 0.1µm pore size; White Beeswax BP/EP (Seatons) in the form of white pellets; Carnauba wax, refined, No 1, yellow (CAS-No. 8015-86-9, Acros Organics) in the form of yellow flakes; toluene (Chromasolv grade, Sigma Aldrich), cyclohexane (Laboratory Reagent grade, Sigma Aldrich). A “leaf sample of *Copernicia prunifera* 20010753” was received as a gift from Katie Tresedes of the Eden Project, Cornwall (www.edenproject.com).

2.2 Preparation of wax coated filter papers

2.2.1 Dip coating

A filter paper was dipped into 2.0% solution of beeswax (or carnauba wax) in toluene for five minutes and then air dried. For double dipped membranes, the filter paper was redipped for a further five minutes being allowed to air dry again.

2.2.2 Spin coating

A spin coater (Laurell WS-400BH-6NPP-Lite) was used. To apply the wax, a filter paper was attached (at the edges) to a microscope slide to hold the filter paper during spin coating. Initially 2.0% solutions of beeswax and of carnauba wax (both in toluene) were used drop wise but these were found to be unreproducible. A micro pipette was found to work better although, surprisingly, the toluene was slow to evaporate, perhaps because of the porous nature of the filter paper (see later). So other solvents with a lower boiling point, which were readily available, were tested for solubility and cyclohexane was chosen to make up 2.0% solutions of beeswax and of carnauba wax. The spinning conditions were 2000rpm for 1 min with the 2.0% wax (beeswax or carnauba) in cyclohexane solution being added in 50µl aliquots a few seconds apart. Two aliquots were found (by SEM, not shown) to give patchy coverage but three aliquots was found to be give good coverage, and this is what was used.

2.3 Diffusion Apparatus

2.3.1 Description

A diffusion apparatus was set up to test the diffusion of the membranes (Figure 1), similar to that described elsewhere [14,15] and consists of two identical sides A and B and an interface (port) in-between the two cells. Each cell was, internally, 7.6 cm long by 5.0 cm wide by 5.5 cm high. The internal diameter of the mass transfer hole was 1.5 cm, with the hole starting 1.5cm above the base, giving a minimum volume of 114cm³. The test volume used was ~161cm³.

The interface consists of two rubber rings (outer diameter=2.5cm) which hold the membrane-between them before bolting the whole system together. Lids were used to avoid evaporation of the liquids.

2.3.2 Operation

The apparatus is assembled with the membrane being investigated put in place between the two cells. The fluorescein solution ($\sim 1.37 \times 10^{-03}$ mol/dm³ (accurately measured)) is placed into cell A with cell B filled with deionised water. In both cases ~ 160 cm³ (accurately measured) was used. The solutions were stirred using magnetic stirrers (just visible in Figure 1). The apparatus was left at ambient conditions and the diffusion of the fluorescein followed by periodically sampling both cells and determining the concentration of the fluorescein by UV/vis spectrometry. Apart from sampling, the cells were left with their lids on to reduce solvent evaporation. At the end of some experiments the volumes of the solutions in each cell were measured.

To investigate the resistance of the diffusion apparatus, a diffusion experiment was performed but without a membrane fitted at the interface, ie a “blank”. To do this a glass microscope slide was placed in each cell blocking the approach to the transfer hole, before the addition of the solutions into each cell. The glass slides were removed to start the experiment. The same procedure of measuring the absorbance after certain time intervals was used except that readings were taken every minute due to rapid mixing. The mixing was too quick to enable it to be followed, so the experiment was repeated using a fluorescein solution with 10% concentration of that normally used, which did enable it to be followed.

Each membrane coating condition was measured twice and the results averaged apart from the blank experiment which was only run once.

2.4 UV/vis

A Ultraviolet-Visible (UV-Vis) spectrophotometer (Agilent 8453, Agilent Technologies) with Agilent Chemstation software was used to measure the absorbance of the fluorescein sodium salt and sample solutions.

A fluorescein calibration curve was constructed to enable absorbance-concentration conversions. The extinction coefficient was found to be $36115 \text{ M}^{-1} \text{ cm}^{-1}$ at 490 nm (assuming 100% pure product) and was used.

2.5 Contact angle

Contact angle was measured using a CAM200 Contact Angle & Surface Tension Meter (KSV Instruments). For each sample three measurements were made, with each measurement being the average of left and right contact angles.

2.6 X-ray Diffraction (XRD)

XRD measurement were carried out using a Philips XPert instrument with $\text{CuK}\alpha$ radiation ($\lambda=0.15404$ nm), a Cu anode, a voltage of 40 kV, a current intensity of 40 mA and a Ni filter. The scans were collected between $2\theta=4^\circ$ and 60° with a scanning speed of 2° min^{-1} .scan (ie 0.05 deg step width).

The WAXS patterns were also used to determine the unit cell parameters, the d-spacing (d_{hkl}), using Bragg's law [16]:

$$2d_{hkl}\sin\theta = n\lambda$$

Equation 1

where, λ is the X-ray wavelength, θ is half of the 2θ position of the centre of the respective crystalline peak, and n is an integer ($n=1,2,3,\dots$) depending on the order of the given plane related to the respective peak.

XRD analysis assumes a perfectly flat surface. As the samples were mostly porous (as shown by SEM, Section 3.2.3) they did not have a perfectly flat surface. This causes slight misalignment of the samples in relation to the X-ray beam with the possible consequence of small differences with that of previously reported peaks of wax samples.

2.7 Scanning Electron Microscope (SEM) analysis

Samples of filter paper (coated and uncoated) as well as a leaf of *Copernicia prunifera* was examined using SEM. The coated filter papers were examined on their coated surface. The leaf was used as received, ie it had been allowed to air dry naturally. Four portions of leaf were examined: each filter paper or leaf portion was mounted on an aluminium stub with carbon tab and coated in gold for 4 minutes using a sputter coater (EMSCOPE SC500), before being examined on a Zeiss EVO MA15 SEM.

2.8 Differential Scanning Calorimetry (DSC)

DSC was measured using a Perkin Elmer DSC 8000 instrument, with scanning from 10 to 150°C at 10°C/min.

2.9 Absolute density

A MicroMeritics AccuPyc 1330 Pycnometer was used to determine absolute density of beeswax and carnauba wax. Each measurement is the average of five repeat runs. The results were: beeswax 0.9520 ± 0.0004 (g/cm³) and carnauba wax 1.0011 ± 0.0001 (g/cm³). Each filter paper was weighed using an analytical balance before and after each coating in order to calculate the amount of wax deposited on the filter paper and hence, using the measured absolute density, to calculate the coating thickness.

3. Results and discussion

3.1 Diffusion experiments

3.1.1 Apparatus blank (i.e. diffusion apparatus without a membrane)

To investigate the resistance of the diffusion cells, a diffusion experiment was performed but without a membrane fitted at the interface, i.e. a “blank”. The diffusion of fluorescein solution in one cell ($\sim 1.37 \times 10^{-3}$ mol/dm³ i.e. the same as that used for the other diffusion experiments) and water in the other cell was too quick to enable the change to be followed, so the experiment was repeated using a fluorescein solution 10% of that previously used, which did enable it to be followed (Figure 2a). This indicates that the diffusion time is much too short for the normal solution so it cannot be “resolved” using current methods i.e. taking a sample is on the order of the diffusion time.

3.1.2 Paper blank (i.e. diffusion apparatus with only an untreated membrane)

To investigate the resistance of the filter paper (0.1µm pore size) on the diffusion between the cells, diffusion experiments were performed using only a membrane fitted at the interface, a “paper blank”. (Note though this actually measured the combined effect of the apparatus blank and filter

paper, something which is corrected for (see later).) The diffusion of fluorescein and water was monitored over a period of 1500 minutes (Figure 2b) at which point it had reached equilibrium concentration. Both initial and repeat experiments gave similar results and showed that the experiment was reproducible.

3.1.3 Single dipped beeswax

The effect of using filter paper dipped into 2% was investigated, over a period of 12,000 minutes (Figure 2b). Both initial and repeat experiments gave very similar results. Comparing this data with later figures (eg Figure 2c) when longer times were used revealed that equilibrium was obtained after ~6000 minutes (rather than the data points becoming more noisy after 6000 minutes).

3.1.4 Double dipped beeswax

The effect of using filter paper double dipped into 2% beeswax was investigated over a period of 12,000 minutes (Figure 2b). Both initial and repeat experiments gave similar results. The rate of diffusion was slower than for the single dipped beeswax, and had still not reached equilibrium after 12,000 minutes. This could be because the second coating had covered the unfilled pores from the single coat. This suggestion is supported by the increase in ~~mass~~ average wax thickness from single coat (4.8 μ m) to double coat (6.5 μ m) (Table 1). Such a small increase in thickness would not explain such a big reduction in permeability alone.

3.1.5 Single dipped carnauba wax

The effect of using filter paper dipped into 2% carnauba wax was investigated over a period of 10,000 minutes (Figure 2c). Both initial and repeat experiments gave very similar results. Equilibrium was obtained after ~6000 minutes.

3.1.6 Double dipped carnauba wax

The effect of using filter paper double dipped into 2% carnauba wax was investigated over a period of 10,000 minutes (Figure 2c). Both initial and repeat experiments gave similar results. The rate of diffusion was much slower than for the single dipped carnauba wax, and had still not reached equilibrium after 10,000 minutes. This could be because the second coating had covered unfilled pores from the single coat. This suggestion is supported by the increase in average wax thickness from single coat (3.4 μ m) to double coat (13.7 μ m) (Table 1).

3.1.7 Spin coated beeswax

In order to try to get a better coverage of wax onto the filter paper spin coating was tried as the application method, using 2% beeswax. Diffusion was followed over period of 12,000 minutes (Figure 2d). Both initial and repeat experiments gave very similar results. Equilibrium was obtained after ~6000 minutes.

3.1.8 Spin coated carnauba wax

The effect of using filter paper spin coated with 2% carnauba wax in cyclohexane was investigated. The diffusion was followed over period of 20,000 minutes (Figure 2d). Both initial and repeat experiments gave similar results. The rate of diffusion was much slower than for the spin coated beeswax, having hardly changed after 12,000 minutes, indicating that the treatment had provided very good coverage/protection.

3.1.9 Comparison of wax and coating techniques

The concentration gradient from the (initial) concentration versus time experiments was used as the diffusion rate (Table 1). Fick's Second Law (Equation 2) was used to convert this into permeability:

$$P = [DH] = \frac{j_i l}{\Delta c} + \frac{\beta \left(\frac{dc}{dt}\right) * x}{\Delta c} \quad \text{Equation 2}$$

Where case dc/dt will be the measured diffusion rate and, x , is the membrane thickness (the thickness of an untreated filter paper, 0.1 mm, was used for all calculations including the blank experiment because it was assumed that the permeability of the wax would be so high that the influence of the 0.1mm filter paper would be negligible), Δc , is the initial difference in concentration across the membrane, and β is a physical constant containing the dimensions of the cell and the membrane. A porous filter paper was used to support the wax layers as the thickness of the wax layers (1-10 μ m) was too low to have sufficient mechanical strength on its own.

However, the permeability values obtained are actually composite as they take into account the combined effects of the permeability of the diffusion apparatus, filter paper and wax coating (if used). To calculate the permeability of the individual components, the experimental permeabilities were converted to resistances then the individual resistance (e.g. blank, filter paper) were subtracted from the total resistance (e.g. blank + filter paper + wax) to give the desired resistance which was then converted into the desired permeability. (It should be noted that the resistance, R , is the reciprocal of the calculated permeability.)

$$R_T = R_1 + R_2 + R_3 \dots \quad \text{Equation 3}$$

The concentration gradient from the (initial) concentration versus time experiments were used to calculate the permeability of the wax coatings (Table 1), and the filter paper support, which is shown to be significantly higher than the wax layers. Also in Table 1 is the ratio of permeability to untreated filter paper, and the "average" wax thickness coating which was calculated by weighing the samples before and after coating. Two methods of coating were investigated: dip coating and spin coating.

A single dip with beeswax gives a wax layer of 4.8 μ m and an effective permeability of 3.141 $\times 10^{-10}$ m²/s, whilst double dipping increases the thickness to 6.5 μ m (a 36% increase) and causes the permeability to decrease to 0.856 $\times 10^{-10}$ m²/s (a 73% decrease). If the double dipping increased the thickness of the wax uniformly then the resistance for the wax should have increased proportionally, assuming no impact on porosity. As the impact of double dipping was greater (36% verses 73%) then the porosity must have changed. This supports the assumption that the single dip coat left patches of uncovered holes on the surface through which the dye solution could diffuse, whilst performing a second dip ensured that most holes in the surface were covered up (see SEM later). Interestingly, spin coating gave a wax layer of 4.5 μ m (which was similar to the single dip coated) and an effective permeability of 2.705 $\times 10^{-10}$ m²/s which is similar to the single dip coated.

A single dip with carnauba wax gives a wax layer of 3.4 μ m and an effective permeability of 3.966 $\times 10^{-10}$ m²/s, whilst double dipping increases the thickness to 13.7 μ m (a 309% increase) and causes the permeability to decrease to 0.043 $\times 10^{-10}$ m²/s (a 99% decrease). If the double dipping increased the thickness of the wax uniformly then the resistance for the wax should

have increased proportionally, assuming no impact on porosity. As the impact of double dipping was less (99% versus 309%) then the porosity must have changed. This supports the assumption that the single dip coat left patches of uncovered holes on the surface through which the dye solution could diffuse, whilst performing a second dip ensured that most holes in the surface were covered up (see Section 3.2.3 SEM). Interestingly, spin coating gave a wax layer of 4.0 μm (which was similar to the single dip coated) and an effective permeability of $0.003 \times 10^{-10} \text{ m}^2/\text{s}$ which is even lower than the double dip coated.

Comparing beeswax with carnauba wax (Table 1) reveals that a single dip for each provides approximately the same resistance to permeability, and whilst double dipping reduces the permeability further for both, the effect is much more noticeable for the carnauba coated samples. The use of spin coating produces a large difference between beeswax and carnauba. Whilst the beeswax spin coating produces a permeability similar to single dipping, the carnauba produces a very low level of permeability.

Table 1 enables the calculated average wax thickness for the different samples to be compared with effective permeability (Figure 3). There is an approximate correlation between thickness and permeability for the wax coated samples, agreeing with Fick's Law, although the lowest permeability covers a wide range of thicknesses. This suggests that the wax is distributed differently between these samples (see Section 3.2.3 SEM).

A number of investigators have researched the permeability of lipid films (eg [2-4,7]) including the use of beeswax and carnauba wax. Donhowe and Fennema [2] found that for both oxygen and water permeability carnauba wax has lower values than beeswax which agrees with the present work. In addition it is interesting to comment on the wax film. The wax layers were formed [2] by casting molten wax onto a dried film of methycellulose and then dissolving away the methycellulose film, resulting in minimum thickness of 40-50 μm ie about ten times the levels in the current work. Even thicker films (264-303 μm) were used by Bourlieu et al [3]. These values are considerably higher than microcapsules, where core plus shell are less than 100 μm , highlighting the need for thin films. Hoa *et al* [17] investigated coating formulations for the beneficial effects on the shelf life of mangos and observed that, of the coatings tested, only the one which had carnauba wax as principal component was an effective water loss barrier under conditions of high relative humidity. Indeed there are commercial fruit coatings (Primafresh 30 and Natural Zivdar) which include carnauba wax [18].

The effect of natural wax present on fruit has also been observed eg apples [6]. The diffusion coefficients of three cultivars show an order of magnitude difference between two cultivars for wax layers of similar thickness (2.5-4 μm), while being much lower than that reported for beeswax [3]. It has been suggested that the difference between the two cultivars might be due to more surface cracking and lenticels or to differences in chemical wax composition between those cultivars [6].

3.2 Physio-chemical examination filter papers /membranes

The diffusion experiments have clearly shown a large variation in permeability between different coatings. However, the amount of wax only partly explains why. To gain an understanding of the physical and /or chemical reasons responsible an examination of the structure of the coatings was undertaken using contact angle, XRD, SEM and DSC.

3.2.1 Contact angle

The contact angle of spin coated samples was measured. Both samples were hydrophobic having angles $>90^\circ$, although beeswax (109.5 ± 6.8 deg) was slightly higher than carnauba wax (96.4 ± 6.1 deg). The values are similar to those reported before for white beeswax (98 ± 4) [3] and carnauba wax (98°) [19] and untreated carnauba straw (98°) [20], which was attributed to the presence of a wax layer on the straw surface. The similarity in the contact angles indicate that both waxes have a similar degree of wettability ie similar force balance between adhesive and cohesive forces.

3.2.2 XRD

X-ray diffraction (XRD) was performed on the spin coated samples in order to better understand the bulk structure of the wax.

The XRD shows that both the beeswax and carnauba wax are crystalline (Table 2 and Figure S1). Two strong diffraction peaks are evident at 3.76 \AA (020) and 4.18 \AA (110), which is characteristic of hydrocarbon chain packing in the orthorhombic crystal system [5]. Thus, beeswax is at least partially crystalline, however, the crystal size is obviously quite small, allowing for tight packing of individual crystallites. It is likely that this type of crystalline morphology accounts, in part, for beeswax being a particularly effective barrier to water diffusion. However, the low concentration of polar constituents in beeswax is, undoubtedly, an important factor as well, since the permeability of gases and vapours is partially governed by the solubility of the penetrant in the film matrix [5].

The XRD pattern of beeswax has been observed before [2, 5, 21-26] with the peaks reported at $3.72 - 3.73$ and $4.1-4.14 \text{ \AA}$ [2, 5, 21, 27]. The small difference is likely to be due to slight misalignment of our samples (see Section 2.6). In addition, Basson and Reynhardt [22] found that the XRD patterns of beeswax and Fischer-Tropsch wax were identical and so decided that beeswax also forms orthorhombic crystals with the chains parallel to the c-axis.

The XRD pattern of carnauba wax has been observed before [2, 10, 23, 25] with the peaks reported at 3.73 and 4.13 \AA [10] compared with our findings of 3.76 and 4.19 \AA (Table 2). Again, the small difference is likely to be due to slight mis-alignment of our samples. Electron diffractions study by Dorest found that carnauba wax appeared to be less ordered than beeswax although the difference decreased on annealing [28,29]. Basson and Reynhardt [10] found that since the XRD patterns of carnauba wax and Fischer-Tropsch wax were almost identical the unit cell of carnauba is most probably also orthorhombic.

Overall, comparing XRD for beeswax and carnauba wax reveals similar crystalline structure, characteristic of orthorhombic structure, and consequently the difference in permeability is not due to crystal structure of the wax.

3.2.3 SEM

SEM images of untreated and treated filter papers are shown in Figure 4. These are all at the same magnification to aid comparison. For each sample a range of magnifications is shown in the supplementary information (Figures S2-S7).

Untreated filter paper (Figure 4a) has a very porous nature with holes $\sim 1 \mu\text{m}$. With beeswax single coated filter paper using low magnification the surface appears smooth with some peaks sticking out but further magnification (Figure 4b) shows that the surface is a mix of small holes, a flat coating of beeswax and a few little peaks. The addition of a second dip has the effect (Figure 4d) of filling in most (but not all) of the holes and adding a few more peaks to

the surface. The decrease in holes would help explain the decrease in permeability of the second dipped filter paper (Table 1).

With carnauba wax single coated filter paper using low magnification the surface appears smooth with some lumps (composed of platelets) sitting on the surface but further magnification (Figure 4c) shows that the filter paper is still very porous (possibly with thin covering around individual fibres) with occasional piece of wax. The addition of a second dip has the effect (Figure 4e) of covering the surface of the filter paper with small lumps of platelets (cf shape of flower petals) but underneath the platelets, most (but not all), of the holes are filled in. The decrease in number of holes would help explain the decrease in permeability of the second dipped filter paper (Table 1). It has been reported [4] that when lipids crystallise as platelets, and these platelets are orientated approximately normal to the direction of vapour flow, resistance to vapour flow is usually great. It would be reasonable to assume that a similar situation is occurring here.

Spin coating wax onto filter paper produced different results. With beeswax (Figure 4f) the surface was smooth (with a wavy effect, that look like “worms”, ~1 µm wide by several µm long) but with no obvious holes. This is consistent with that previously reported [2] but contrasts with the second dip coated sample, which had more holes but slightly lower permeability. This might be because the SEM shows the appearance of the coating and how waxes solidify but does not give a 3D picture showing the location of holes throughout the structure.

With carnauba wax (Figure 4g) the surface was covered with many rippled parts peaking in a platelet, as well as an occasional indentation (possibly sheltering a hole). This appears rougher than that previously reported [2,20] but fits with the second dipped sample, having both better coverage and lower permeability.

The interesting pattern shown by the double dip coated carnauba wax (Figure 4g) raised the issue as to whether the wax was following the pattern that naturally occurred in nature. To test this out a leaf from *Copernicia prunifera* was obtained and examined by SEM (Figure 6). (The leaf was untreated apart from having air dried naturally.) The same range of magnifications has been used in order to aid comparison. There is a noticeable difference in-between the top and underneath of the leaf. Underneath the leaf there appears to be “furrows” (~40µm wide) which are made up of protruding platelets (~40µm wide) with straight edges. There also appears to be strands across the surface possibly arising through fungus impurities. The top side of the leaf, whilst also having variations in height, is smoother with less pronounced features. In addition there appears to be a lack of protruding platelets although the presence of strands (possibly from fungus) and spheres (possibly from pollen) are present. Figure 6e,f show the ridge from underneath the leaf and is a mix of the normal underneath and top leaf images – having some structure and some platelets but less than the rest of the underneath side. This might have arisen from being exposed and being subjected to weathering.

It is known that plant surfaces show an enormous variety of functional three-dimensional structures in the micro-dimension [21, 23, 30]. Epicuticular waxes (plant waxes embedded into the cuticle) often form two- and three- dimensional structures, in dimensions between hundreds of nanometres and some micrometres. The types of structures seen include wax chimneys (*Heliconia collinsiana*), tubules (*Eucalyptus gunnii*), wax platelets with straight edges (*Aloe porphyrostachys*) and coiled rodlets (*Chrysanthemum segetum*) [21, 23, 30].

The SEM of the leaf from *Copernicia prunifera* (Figure 6b) showed a different structure to recrystallized carnauba wax (double dipped) (Figure 5e). This behaviour has been observed

before, namely that certain waxes crystallise in different forms depending on the conditions (e.g. *Juniperus communis* where “nonacosanol” wax tubules in nature recrystallized to form sponge-like curled membranes [21]). This might be explained by the recrystallization conditions on plant surfaces being unique, as the wax molecules move relatively slowly from inside of the leaf through the cuticle and crystallise without a solvent on the dry surface [21]. The only SEM of carnauba that we know of is for “carnauba straw” [20] which would appear to be the leaves after the wax has been removed (by shaking) although it is not specified. The straw shows the presence of fibrils and globular marks, although the low magnification used and the lack of description i.e. whether it is the top or underneath the leaf, makes it difficult to compare directly with the images in Figure 15.

Overall SEM reveals the progression from a very porous structure in untreated filter paper to partial coverage with some permeability upon the addition of some wax, which is as expected. However, subsequently adding more wax (either by double dipping or by using spin coating) has a different effect, depending on the wax used. With beeswax, “complete” coverage still allows for permeability, whereas, with carnauba wax, “complete” coverage gives very low permeability. This indicates not just that the level of coverage has an effect on permeability but also that the composition of the wax used has an effect i.e. a “solid” layer of beeswax is still porous.

3.2.4 DSC

The thermal properties of beeswax and carnauba wax were determined by differential scanning calorimetry (DSC) (Table 3).

Beeswax has a melting point at 64.20°C with a solid-solid (s-s) transition at 53.58°C (Table 3) Other reported melting points vary: Donhowe and Fennema [2] reported 62.0 ± 0.1 °C with an s-s transition at 52°C; Basson and Reynhardt [22] found that beeswax (*mellifera adansonii*) exhibited a wide melting transition consisting of two partially resolved peaks, with the melting process starting at approximately 300 K (27C) and the two peaks occur at 329 K (56°C) and 337 K (64°C); Nikolova *et al* [25] found for heating program 64.62 °C (onset) with 69.72 °C (maximum), and for cooling program 63.48 °C (onset), 51.59 and 61.53 °C (maximum); whilst Buchwald *et al* [31] studied the melting properties for the waxes of several bees - *Apis*, *Bombus*, *Melipona*, *Nanotrigona*, *Plebia* and *Trigona* species and found for *Apis mellifera* (which was the type used in the experiments reported here) that onset ranged from 35.2 ± 0.50 to 40.4 ± 0.72 °C, end ranges from 66.5 ± 0.22 to 70.5 ± 0.46 °C; peak 63.5 ± 0.29 to 68.6 ± 0.46 °C.

Beeswax was found to have an enthalpy of melting (ΔH_f) of 171.53 J/g (Table 3) compared with $158 + 5$ J/g [2], heat of fusion 170.7 ± 4.48 J/g [30], 206.9 J/g (heating program) and -159.2 J/g (cooling program) [25] whilst Buchwald *et al* [31] studied the melting properties for the waxes of several bees found a range for *Apis mellifera* of 117.9 ± 11.83 to 170.7 ± 4.48 J/g.

Carnauba wax has two melting points – indicating a mix – a minor one at 64.11 °C and the main one at 84.44 °C with a solid-solid transition at 78.15°C (Table 3). Other reported melting points vary: Donhowe and Fennema [2] reported 81.7 ± 0.3 °C with two s-s transitions, one at 57°C and the other at 75°C; while Basson and Reynhardt [10] found that the melting of the wax starts at approximately 338 K (65°C) and is complete at approximately 363 K (90°C) with a solid solid transition at 335 K (63°C) when the sample is heated. Carnauba wax was found to have an enthalpy of melting (ΔH_f) 211.24 J/g compared with 196 ± 4 J/g [2].

As waxes have a broad melting range it indicates they are composed of a mixture of compounds. Overall, the thermal properties of the beeswax and carnauba wax used lie within

the (wide) range expected indicating that they are typical of their respective type of wax. It is also clear that carnauba wax has a higher melting point than beeswax indicating differences in chemical composition.

3.3 Chemical composition waxes

Comparing manufacturers' specifications (Table 4) and literature data for beeswax [34-42] (Table S1) and carnauba wax [10,43-55] (Tables S2, S3) enables comparison of the composition of beeswax and carnauba wax:

- i) The **melting point** (Table 4) of carnauba wax (84.5°C) is higher than beeswax (63°C) (This is similar to the DSC results (Table 3) with carnauba wax 84.44°C and beeswax 64.20°C.) Carnauba wax is less pliable than beeswax as it contains high-melting point components in higher proportion [2]. It is likely that the hardness (lack of low-melting point components) of carnauba wax enhances its resistance to gas transmission.
- ii) The **saponification value** of beeswax (89.71) and carnauba wax (86.8) is similar, indicating that the average molecular weight (or chain length) of the fatty acids present is similar. In general, the rate of water transfer across a lipid film increases as the lipid hydrocarbon chain length is decreased and the degree of unsaturation or branching of acyl chains is increased [4]. This occurs because lateral packing of acyl chains is less efficient, causing a reduction in van der Waals' interactions and an increase in hydrocarbon chain mobility. These molecular effects accelerate water transport by elevating the effective H₂O diffusion constant and by increasing the solubility of water in the lipid membrane [4]. As the saponification value is similar then it means that the difference in permeabilities observed is not due to difference in chain length. (It should be noted that direct comparison of average chain length is difficult due to the difference in the way the published values of beeswax and carnauba wax are presented.)
- iii) The **acid value** (a measure of the amount of carboxylic acid groups in a wax) of beeswax (18.42) is much higher than carnauba wax (4.2). The increased carboxylic acid groups in beeswax could contribute to the greater permeability of beeswax as it has been reported that polar groups in a lipid film sorb water vapour, thereby assisting moisture migration through the film [4]
- iv) The amount of **hydrocarbon** is much higher in beeswax (14%) than carnauba wax (~1%). Beeswax contains a small amount of unsaturated hydrocarbons, and these hydrocarbons are responsible for its flexibility [2] and have been reported to facilitate diffusion of oxygen through beeswax film [2].
- v) **Cinnamic acid** esters are absent from beeswax but present in significant quantities in carnauba wax. It is believed that the cinnamic esters are mainly responsible for the unusual properties attributed to carnauba wax [51, 55], although they did not elaborate.

Comparing the composition of beeswax and carnauba wax indicates that whilst some factors are similar (e.g. average chain length) there are a number of others which are different with beeswax having increased hydrocarbons and carboxylic acid groups, and carnauba wax having the presence of significant quantities of cinnamic acid esters. Consequently, the differences in the permeabilities among the wax films are attributed to the increased hydrocarbon and carboxylic acid groups present in beeswax facilitating water transfer.

This type of behaviour has been reported before [6], when differences in chemical wax composition between apple cultivars has been suggested as a possible cause for the difference in their diffusion coefficient. This leads to the possibility of being able to develop better commercial coatings for fruit by controlling the permeabilities of wax through the addition of specific chemical compounds.

3.4 Volume change phenomena

During the course of the experiments using the diffusion apparatus, it was observed that the level of liquid in the two cells was not equal at the end of the experiments (e.g. Figure 6). This section reports on the observations made and suggests reasons, although, as this was not anticipated, the apparatus was not designed to monitor this (e.g. it was not graduated so continuous monitoring was not possible) so the results are regarded as preliminary but interesting.

During the course of the diffusion experiment using single dipped beeswax filter paper it was observed that the volume of the two cells was uneven at the end and the two liquids were weighed (Table 5). Both cells (fluorescein and water) started with 162g. For the “fluorescein” cell there was a net increase of ~17g whilst the “water” cell had a net loss of ~34g, resulting in an overall loss of ~16g, which was presumably due to evaporation eg when the cells were being sampled, and works out as ~1g per cell per day, which does not seem excessive. This volume change phenomena was also observed for the double dipped beeswax (which was being run at the same time), although the change occurred at a different speed. For the single dipped beeswax a noticeable change appeared after 3-4 days but it took more than 8 days for the double dipped change to become noticeable.

Now that this phenomenon was apparent more attention was paid to it during the experiments using the spin coated filter papers (Table 5). The beeswax coated samples had the same behaviour as the dip coated beeswax. However, for the carnauba wax spin coated samples both “fluorescein” and “water” cells lost liquid, albeit with more coming from the “water” cell. This difference might be due to the very low permeability of spin coated carnauba wax samples (Table 2) meaning that there was an almost impervious barrier present, with water loss due to evaporation being a larger factor than anything else.

Initially the possibility of this being Reverse Osmosis was considered but there was no external pressure available to make this function. Instead it appears to be an example of Forward Osmosis (FO), which is driven by osmotic pressure difference across a semipermeable membrane [58-63]. The selection of an appropriate membrane and “draw” solution is crucial for the process efficiency [59]. A large range of materials have been reported as suitable for use as membranes [58, 60, 64] and deionised water is already known to be used as a “feed” solution [61], so it would appear that the combination of the filter paper used here (hydrophilic PVDF) coated with beeswax experiences FO with fluorescein solution (as “draw” solution) even at the low concentration used ($\sim 1.37 \times 10^{-3}$ M), and deionised water (as feed solution). Calculating the flux value (Table 5) produced a value of $\sim 0.5 \text{ Lm}^{-2}\text{h}^{-1}$. The role of carnauba wax is uncertain. It might be that the wax (on these spin coated samples) so blocks up the pores that the filter paper can no longer be considered as semi permeable, and so does not experience FO.

Clearly this is an area in which more investigation is needed. However, these preliminary results are presented in order increase knowledge on the subject.

It should be noted that this change in volume phenomena meant that the underlying assumption in the fluorescein concentration calculations ie that the levels of the two cells remained constant during an experiment, is not correct. However as the permeability values were calculated using initial rates of diffusion (ie the rate before the concentration reached equilibrium) then it should only have a small effect on the absolute values and no effect on the relative values.

4 Conclusions

A diffusion cell was used to investigate the permeability of fluorescein solution through thin solid wax coated filter paper. On the scale of the dye material the surface structure can be very porous and allows for effective permeability. Two waxes (beeswax and carnauba wax) and two coating methods (single or double dipping, and spin coating) were investigated.

Results indicate that both the wax material itself and the sample preparation is extremely important to the structure and the resulting permeability of the membranes. Spin coating was much more effective than dip coating in reducing permeability. Carnauba wax had a much lower permeability than beeswax which is attributed to its different chemical properties. The differences in the permeabilities among the wax films are attributed to the increased hydrocarbon and carboxylic acid groups present in beeswax facilitating water transfer [2,4]. This leads to the possibility of being able to develop better commercial coatings for fruit by controlling the permeabilities of wax through the addition of specific chemical compounds.

SEM showed that the single dip coat left patches of uncovered holes on the surface through which the dye solution could diffuse through, whilst performing a second dip ensured that most holes (beeswax), or almost all holes (carnauba wax) in the surface were covered up. The results indicate that, care should be taken in the control of the solidification step as this could strongly influence the structure, and hence permeability of any resulting solid membrane. Future work could investigate the impact of the speed of cooling as well as incorporation of additives to control crystallisation structure. Since this is a crystallisation process then incorporation of seeding to initiate crystallisation as well as cooling rate should be investigated [65].

To test whether double dip coated carnauba wax was following the pattern that naturally occurred in nature, a leaf from *Copernicia prunifera* was obtained and found to show a different structure to recrystallized carnauba wax. This behaviour has been observed before, namely that certain waxes crystallise in different forms depending on the conditions (eg *Juniperus communis*) [21]. Future work will focus on developing means of controlling the structure of wax walls on solidification to better control permeability

During the experimental work a difference in levels between the two cells was observed, which was attributed to differences in osmotic pressure between the cells. This could be further investigated in the future.

Our findings indicate that for thin films (3 – 7 μm) the solidification step could strongly influence the structure. This has relevance to other systems which have layers of wax with similar thicknesses eg microcapsules, and indicates that care should be taken in the control of the solidification step, as this could strongly influence the structure, and hence properties of any resulting solid layer.

5 Acknowledgements

We wish to thank: Katie Tresedes of the Eden Project, Cornwall (www.edenproject.com) for the gift of “leaf sample of *Copernicia prunifera* 20010753”; Mahoulo Ahouansou of SCAPE, University of Leeds, for contact angle measurements; Mohammed Javed of SCAPE, University of Leeds for performing the DSC; Stuart Micklewaite, of Leeds Electron Microscopy and Spectroscopy Centre, SCAPE, University of Leeds for performing the SEM; and Tim Comyn, of SCAPE, University of Leeds for performing the XRD.

This research did not receive any grant from funding agencies in the public, commercial, or not-for-profit sectors.

6 References

1. A Madene, M Jacquot, J Scher and S Desobry, "Flavour encapsulation and controlled release – a review" *Int J Food Sci Tech* 41 (2006) 1–21
2. IG Donhowe and O Fennema, "Water vapour and oxygen permeability of wax films" *J Am Oil Chem Soc* 70 (1993) 867-873
3. C Bourlieu, V Guillard, H Powell, B Vallès-Pàmies, S Guilbert, N Gontard "Performance of lipid-based moisture barriers in food products with intermediate water activity" *Eur J Lipid Sci Tech* 108 (2006) 1007-1020
4. JJ Kester and O Fennema, "Resistance of lipid films to water vapour transmission" *J Am Oil Chem Soc* 66 (1989) 1139-1146
5. JJ Kester and O Fennema, "An edible film of lipids and cellulose ethers: barrier properties to moisture vapour transmission and structural evaluation" *J Food Sci* 54 (1989) 1383 – 1389
6. EA Veraverbeke, P Verboven, N Scheerlinck, ML Hoang, BM Nicolai, "Determination of the diffusion coefficient of tissue, cuticle, cutin and wax of apple" *J Food Eng* 58 (2003) 285–294
7. M Mellema, WAJ van Benthum, B Boer, J von Harras A Visser, "Wax encapsulation of water soluble compounds for application in foods" *J Microencapsul* 23 (2006) 729-740
8. L Schreiber, M Riederer, "Determination of diffusion coefficients of octadecanoic acid in isolated cuticular waxes and their relationship to cuticular water permeabilities" *Plant Cell Environ* 19 (1996) 1075–1082
9. J Milanovic, V Manojlovic, S Levic, N Rajic, V Nedovic and B Bugarski, "Microencapsulation of Flavors in Carnauba Wax" *Sensors* 10 (2010) 901-912
10. I Basson and EC Reynhardt "An investigation of the structures and molecular dynamics of natural waxes: II. Carnauba wax" *J Phys D Appl Phys* 21 (1988) 1429-1433
11. TH Shellhammer, TR Rumsey and JM Krochta "Viscoelastic properties of edible lipids" *J Food Eng* 33 (1997) 305-320
12. S Collins, D York, S Kazmi, AK Mohammed, "The formation of wax walled microcapsules via double emulsion using cross membrane emulsification at elevated temperatures" Manuscript in preparation
13. D Montermini, CP Winlove, CC Michel "Effects of perfusion rate on permeability of frog and rat mesenteric microvessels to sodium fluorescein" *J Physiol* 543.3 (2002) 959–975
14. MI Vazquez, C Torras, R Garcia-Valls, J Benavente,"A study on thermal effect on structure and transport properties of a composite lignosulfonated-polyamide/polysulfone membrane" *Desalination* 245 (2009) 570–578
15. J Benavente, A Muñoz, A Heredia, "Electrokinetic characterization of isolated pepper cuticles in protonic form", *Solid State Ionics* 97 (1997) 89–95
16. N Dencheva, T Nunes, MJ Oliveira, S Denchev "Microfibrillar composites based on polyamide/polyethylene blends. 1. Structure investigations in oriented and isotropic polyamide 6" *Polymer* 46 (2005) 887-907
17. TT Hoa, M-N Ducamp, M Lebrun and EA Baldwin, "Effect of different coating treatments on the quality of mango fruit" *J Food Quality* 25 (2002) 471-486
18. CH Mannheim and T Soffer, "Permeability of different wax coatings and their effect on citrus fruit quality" *J Agr Food Chem* 44 (1996) 919-923
19. PJ Holloway, "Chemistry of leaf waxes in relation to wetting" *J Sci Fd Agric* 20 (1969) 124-128
20. JE Fernandes, TN de Castro Dantas, JLC Fonseca MR Pereira, "Carnauba Straw: characterisation and chemical treatments" *J Appl Polym Sci* 122 (2011) 1614-1621

21. HJ Ensikat, M Boese, W Mader, W. Barthlott, K Koch, "Crystallinity of plant epicuticular waxes: electron and X-ray diffraction studies" *Chem Phys Lipids* 144 (2006) 45-59
22. I Basson and EC Reynhardt "An investigation of the structures and molecular dynamics of natural waxes: I. Beeswax" *J Phys D Appl Phys* 21 (1988) 1421-1428
23. PE Kolattukudy "Plant waxes" *Lipids* 5 (1970) 259-275
24. Y Gaillarda, A Mijab, A Burra, E Darque-Cerettia, E Feldera, N Sbirrazzuolib, "Green material composites from renewable resources: Polymorphic transitions and phase diagram of beeswax/rosin resin" *Thermochim Acta* 521 (2011) 90– 97
25. KR Nikolova, I Panchev, D Kovacheva S Pashova, "Thermophysical and optical characteristics of bee and plant waxes" *J Optoelectron Adv M* 11 (2009) 1210-1213
26. J Brandao-Neto SP Thompson AR Lennie FF Ferreira and CC Tang, "Characterisation of wax as a potential diffraction intensity standard for macromolecular crystallography beamlines" *J Synchrotron Radiat* 17(2010) 53-60
27. D Muscat, R Adhikari, S McKnight, Q Guo, B Adhikari, "The physicochemical characteristics and hydrophobicity of high amylose starch–glycerol films in the presence of three natural waxes" *J Food Eng* 119 (2013) 205–219
28. DL Dorset "Crystallography of waxes – an electron diffraction study of refined and natural products" *J Phys D Appl Phys* 30 (1997) 451-457
29. DL Dorest "Development of lamellar structures in natural waxes – an electron diffraction investigation" *J Phys D Appl Phys* 32 (1999) 1276-1280
30. K Koch, H-J Ensikat "The hydrophobic coatings of plant surfaces: Epicuticular wax crystals and their morphologies, crystallinity and molecular self-assembly" *Micron* 39 (2008) 759-772
31. R Buchwald, MD. Breed and AR Greenberg "The thermal properties of beeswax: unexpected findings" *J Exp Biol* 211(2008)121-127
32. AP Tulloch "Analysis of whole beeswax by gas liquid chromatography" *J Am Oil Chem Soc* 49 (1972) 609 -610
33. AP Tulloch "The composition of Beeswax and other waxes secreted by insects" *Lipids* 5(1970) 247-258
34. AP Tulloch and LL Hoffman, "Canadian Beeswax: Analytical Values and Composition of Hydrocarbons, Free Acids and Long Chain Esters" *J Am Oil Chem Soc* 49 (1972) 696 – 699
35. AP Tulloch, "Beeswax: structure of the esters and their component hydroxyl acids and diols" *Chem Phys Lipids* 6 (1971) 235-265
36. JJ Jiménez, JL Bernal, MJ del Nozal, L Toribio, J Bernal, "Detection of beeswax adulterations using concentration guide-values" *Eur J Lipid Sci Tech* 109 (2007) 682–690
37. AP Tulloch, "Beeswax – composition and analysis", *Bee World* 61 (1980) 47-62
38. AP Tulloch and LL Hoffman "Canadian beeswax: Analytical values and composition of hydrocarbons, free acids and long chain esters" *J Am Oil Chem Soc* 49 (1972) 696-699
39. R Aichholza, E Lorbeerb, "Investigation of combwax of honeybees with high-temperature gas chromatography and high-temperature gas chromatography– chemical ionization mass spectrometry I. High-temperature gas chromatography" *J Chromatogr A* 855 (1999) 601– 615
40. R Aichholza, E Lorbeerb, "Investigation of combwax of honeybees with high-temperature gas chromatography and high-temperature gas chromatography– chemical ionization mass spectrometry II: High-temperature gas chromatography–chemical ionization mass spectrometry" *J Chromatogr A* 883 (2000) 75–88
41. JJ Jiménez, JL Bernal, S Aumente, MJ del Nozal, MT Martín, J Bernal, "Quality assurance of commercial beeswax Part I. Gas chromatography–electron impact ionization mass spectrometry of hydrocarbons and monoesters" *J Chromatogr A* 1024 (2004) 147–154

42. JJ Jiménez, JL Bernal, S Aumente, L Toribio, J Bernal, "Quality assurance of commercial beeswax II. Gas chromatography–electron impact ionization mass spectrometry of alcohols and acids" *J Chromatogr A* 1007 (2003) 101–116
43. L Wang, S Ando, Y Ishida, H Ohtani, S Tsuge, and T Nakayama, "Quantitative and discriminative analysis of carnauba waxes by reactive pyrolysis-GC in the presence of organic alkali using a vertical microfurnace pyrolyzer" *J Anal Appl Pyrol* 58–59 (2001) 525–537
44. A Asperger, W Engewald, G Fabian, "Advances in the analysis of natural waxes provided by thermally assisted hydrolysis and methylation (THM) in combination with GC:MS" *J Anal Appl Pyrol* 52 (1999) 51–63
45. A Asperger, W Engewald, G Fabian "Analytical characterization of natural waxes employing pyrolysis–gas chromatography–mass spectrometry" *J Anal Appl Pyrol* 50 (1999) 103–115
46. AP Tulloch, "Comparison of Some Commercial Waxes by Gas Liquid Chromatography" *J Am Oil Chem Soc* 50 (1973) 367-371
47. CS Barnes, MN Galbraith, E Ritchie and WC Taylor, "Carnaubadiol, A Triterpene From Carnauba Wax" *Aust J Chem* 18 (1965) 1411-22
48. J de Brito Cysne, R Braz-Filho, MV Assunção, DE de Andrade Uchoa, ER Silveira and ODL Pessoa "1H and 13C NMR spectral assignments of four dammarane triterpenoids from carnauba wax" *Magn Reson Chem* 44 (2006) 641–643
49. KE Murray and R Schoenfeld "Studies of Waxes XI. The hydroxyl acids of carnauba Wax" *Aust J Chem* 8 (1955) 437-443
50. KE Murray and R Schoenfeld "Studies of Waxes X. The diols of carnauba Wax" *Aust J Chem* 8 (1955) 432-436
51. LE Vandenburg and EA Wilder, "Aromatic Acids of Carnauba Wax" *J Am Oil Chem Soc* 44 (1967) 659-662
52. KE Murray and H-R Schulten, "Field Desorption Mass Spectrometry of Lipids. I the application of field desorption mass spectrometry to the investigation of natural waxes" *Chem Phys Lipids* 29 (1981) 11-21
53. JF Lawrence, JR Iyengar, BD Page and HBS Conacher, "Characterisation of Commercial Waxes by high temperature gas chromatography" *J Chromatogr* 236 (1982) 403-419
54. DT Downing, ZH Kranz and KE Murray, "Studies in Waxes XX. The Quantitative Analysis of Hydrolysed Carnauba Wax by Gas Chromatography" *Aust J Chem* 14 (1960) 619-627
55. LE Vandenburg and EA Wilder, "The Structural Constituents of Carnauba Wax" *J Am Oil Chem Soc* 47 (1970) 514- 518
56. John L Seaton & Co Ltd, "Seatons White Beeswax Ph Eur", Hessle, Certificate of analysis Batch 9280, March 2011
57. Acros Organics "Carnauba wax, refined, No 1 yellow" certificate of analysis, Lot A0308192 May 2011
58. TY Cath, AE Childress, M Elimelech "Forward osmosis: Principles, applications, and recent developments" *J Membrane Sci* 281 (2006) 70–87
59. N Akther, A Sodiq, A Giwa, S Daer, HA Arafat and SW Hasan "Recent advancements in forward osmosis desalination: A review" *Chem Eng J* 281 (2015) 502–522
60. IL Alsvik and M-B Hägg "Pressure Retarded Osmosis and Forward Osmosis Membranes: Materials and Methods" *Polymers* 5 (2013) 303-327
61. TY Cath, M Elimelech, JR McCutcheon, RL McGinnis, A Achilli, D Anastasio, AR Brady, AE Childress, IV Farr, NT Hancock, J Lampi, LD Nghiem, M Xie, NY Yip "Standard Methodology for Evaluating Membrane Performance in Osmotically Driven Membrane Processes" *Desalination* 312 (2013) 31–38
62. S Zhao, L Zou, CY Tang, D Mulcahy "Recent developments in forward osmosis: Opportunities and challenges" *J Membrane Sci* 396 (2012) 1– 21

63. M Qasim, NA Darwish, S Sarp, N Hilal “Water desalination by forward (direct) osmosis phenomenon: A comprehensive review” *Desalination* 374 (2015) 47–69
64. GM Geise, DR Paul, BD Freeman “Fundamental water and salt transport properties of polymeric materials” *Prog Polym Sci* 39 (2014) 1– 42
65. J Ulrich, HC Bülaü “Chapter7: Melt crystallization” in *Handbook of Industrial Crystallization (Second Edition)*, Editor A S. Myerson, 2002, Pages 161-179. Butterworth-Heinemann

Figure captions

Figure 1 Diffusion apparatus set up at the start of the experiment (with magnetic stirrers just visible)

Figure 2 Concentration profiles for a) apparatus only (using normal concentration and 10% of normal concentration); b) blank (filter paper), single dip coated beeswax and double dip coated beeswax; c) for single and double dip coated carnauba wax; d) for spin coated beeswax and spin coated carnauba wax

Figure 3 Thickness vs permeability for wax coated samples and uncoated filter paper

Figure 4 SEM images for a) untreated filter paper (0.1 μ m pore size), b) single dip beeswax, c) single dip carnauba wax, d) double dip beeswax, e) double dip carnauba wax, f) spin coated beeswax, g) spin coated carnauba wax (all same magnifications) (A larger range of magnifications is shown in Supplementary Information Figures S4-S10)

Figure 5 SEM images of leaf from *Copernicia prunifera*: a) and b) underneath whole leaf (same location different magnifications); c) and d) top whole leaf (same location different magnifications); e) and f) of ridge (underneath whole leaf) (same location different magnifications) (A larger range of magnifications is shown in Supplementary Figures S5-S6)

Figure 6 showing diffusion apparatus at the start (equal height levels) and end (unequal height levels) of a diffusion experiment showing levels in the two cells (left = “water”, right = “fluorescein solution”)

Tables

Table 1 Measurements of wax thickness, initial rate of diffusion and calculated permeability

Table 2 XRD – 2 theta and corresponding values of peaks

Table 3 Thermophysical characteristics of beeswax and carnauba wax

Table 4 Chemical data for beeswax and carnauba wax used (manufacturers certificate of analysis [57, 58])

Table 5 Volume change data for beeswax (single dip coating), beeswax (spin coating) and carnauba wax (spin coating)

Substrate	Average wax thickness (μm)	Initial rate ($\text{mol}^{-1}\text{dm}^{-3}\text{min}^{-1}$)		Experimental Permeability (m^2/s)	Effective Permeability, ($\times 10^{-10}$) (m^2/s)	Ratio of permeability
		rate	R^2			
Apparatus – no filter paper	--	2.3×10^{-6}	0.9773	4.2×10^{-8}	--	--
Filter paper - uncoated	0.0	5.7×10^{-8}	0.9959	8.3×10^{-10}	8.488	1.0000
Beeswax - dip - single coat	4.8	1.2×10^{-8}	0.8746	2.3×10^{-10}	3.141	0.3700
Beeswax - dip - double coat	6.5	4.1×10^{-9}	0.6698	7.7×10^{-11}	0.856	0.1009
Beeswax - spin coat	4.5	1.3×10^{-8}	0.5700	2.1×10^{-10}	2.705	0.3186
Carnauba wax - dip - single coat	3.4	1.4×10^{-8}	0.9199	2.7×10^{-10}	3.966	0.4672
Carnauba wax - dip - double coat	13.7	2.2×10^{-10}	0.7894	4.3×10^{-12}	0.043	0.0050
Carnauba wax - spin coat	4.0	1.5×10^{-11}	0.1363	2.6×10^{-13}	0.003	0.0003

Table 1 Measurements of wax thickness, initial rate of diffusion and calculated permeability

Beeswax		Carnauba wax		Peak assignment	Reference
2 theta	Angstrom	2 theta	Angstrom		
21.2261	4.1819	21.1761	4.1917	<110>	[10,22]
23.6261	3.7622	23.6261	3.7622	<020>	[21,24]
40.3261	2.2345			<200>	

Table 2 XRD – 2 theta and corresponding values of peaks

Characteristic	Beeswax	Carnauba wax
First peak (°C)	53.58	64.11
First peak (mW)	11.0948	5.2040
Second peak (°C)	--	78.15
Second peak (mW)	--	22.4119
Main Peak (°C)	64.20	84.44
Area (mJ)	1286.459	1689.910
ΔH (J/g)	171.5278	211.2388

Table 3 Thermophysical characteristics of beeswax and carnauba wax

Description	White Beeswax		Carnauba wax, refined, No 1, yellow	
Supplier	Seatons (batch 9280)		Acros Organics (lot A0308192)	
	Specification	Result	Specification	Test value
Appearance	n/a	white pellets	Yellow powder or flakes	yellow flakes
Drop point (°C)	61.0 – 66.0	63.0	--	--
Melting point (°C)	--	--	81 to 86	84.5
Acid value (mgKOH/g)	17.0-24.0	18.42	2 to 7	4.2
Ester value	70-80	71.29	--	--
Saponification value (mgKOH/g)	87-104	89.71	78 to 95	86.8

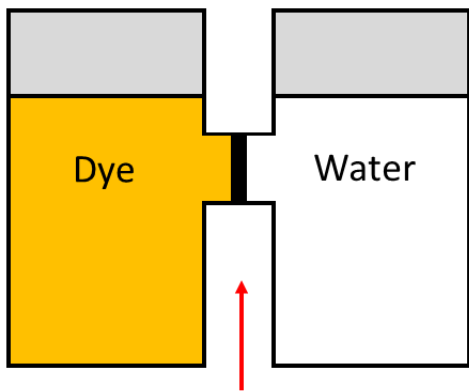
Table 4 Chemical data for beeswax and carnauba wax used (manufacturers certificate of analysis [56, 57])

Factor	Substrate				
	Beeswax single dip coated	Beeswax spin coated	Beeswax spin coated rpt	Carnauba wax spin coated	Carnauba wax spin coated rpt
Fluorescein cell: Initial mass (g)	162.27	160.36	160.02	160.00	160.17
Final mass (g)	179.70	176	185.38	149.67	153.84
Difference (g)	+17.43	+15.64	+25.36	-10.33	-6.33
Water cell: Initial mass (g)	162.47	160.12	160.03	160.00	160.22
Final mass (g)	128.89	134.07	123.19	137.82	143.86
Difference (g)	-33.58	-26.05	-36.84	-22.18	-16.36
Missing (g)	16.15	10.41	11.48	32.51	22.69
Period of time (min)	11465	17000	18780	33000	17240
Overall rate loss per cell (g/day)	1.0142	0.4409	0.4401	0.7093	0.9476
Flux fluorescein sol ($Lm^{-2}h^{-1}$)	0.5156	0.3120	0.4580	-0.106	-0.125

Table 5 Volume change data for beeswax (single dip coating), beeswax (spin coating) and carnauba wax (spin coating)

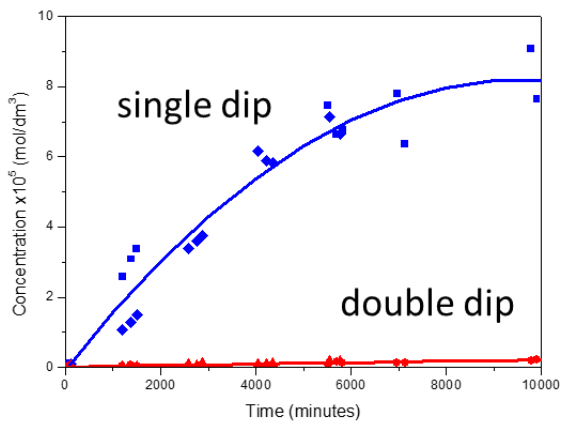
Graphical Abstract

Experiment



Wax membrane
(beeswax or carnauba wax)
(dip coat or spin coat)

Results



Measuring flow of dye through
carnauba wax coated membranes

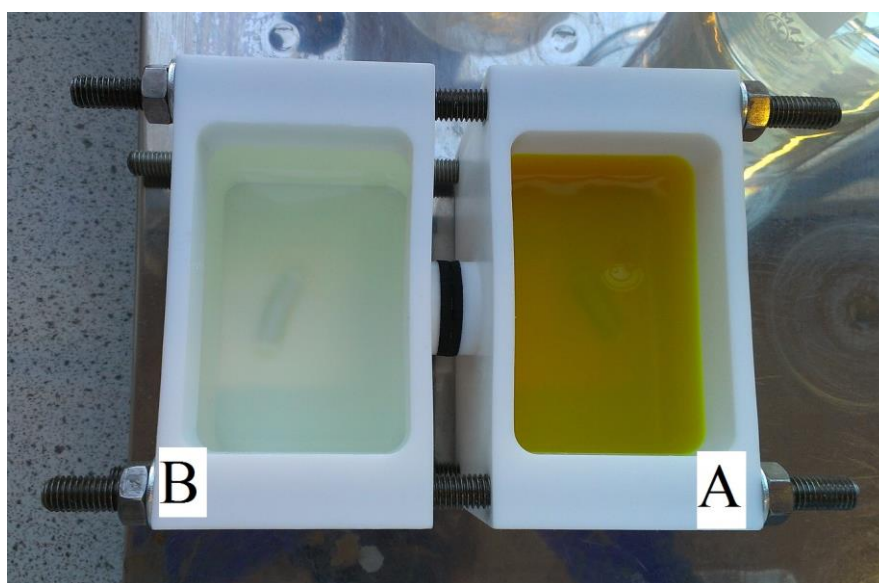


Figure 1 Diffusion apparatus set up at the start of the experiment (with magnetic stirrers just visible)

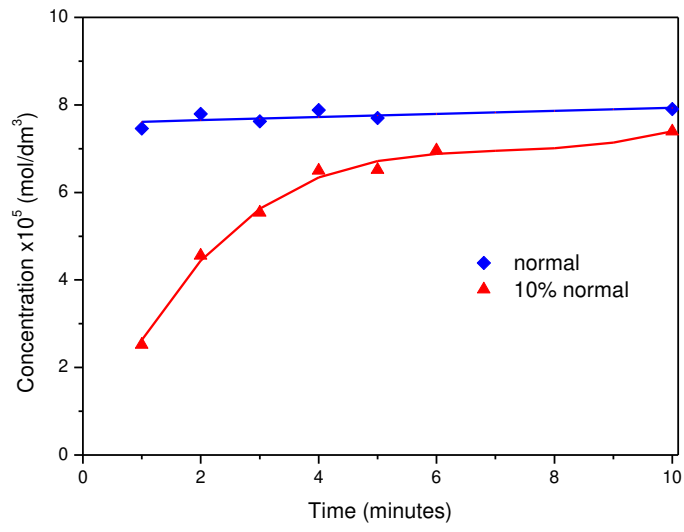


Figure 2a

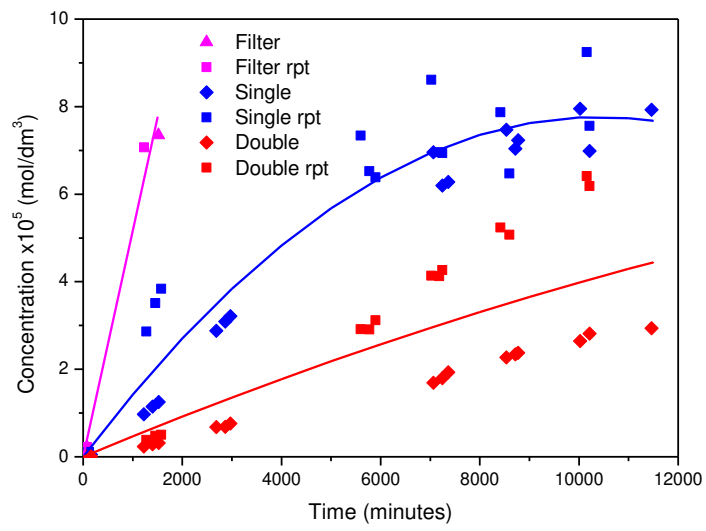


Figure 2b

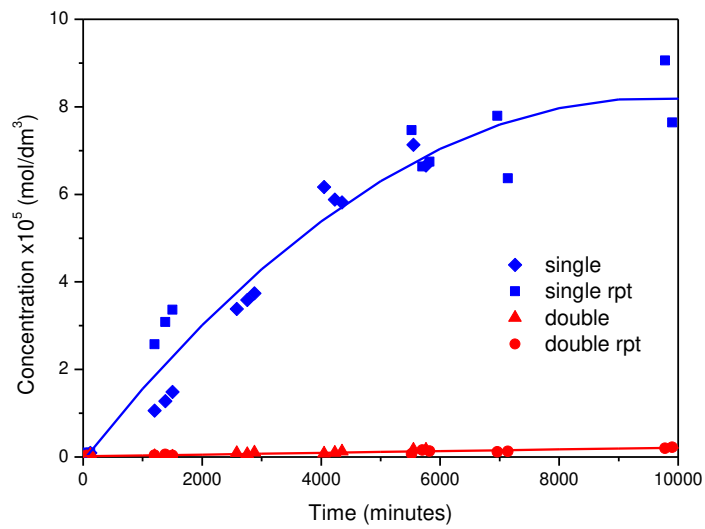


Figure 2c

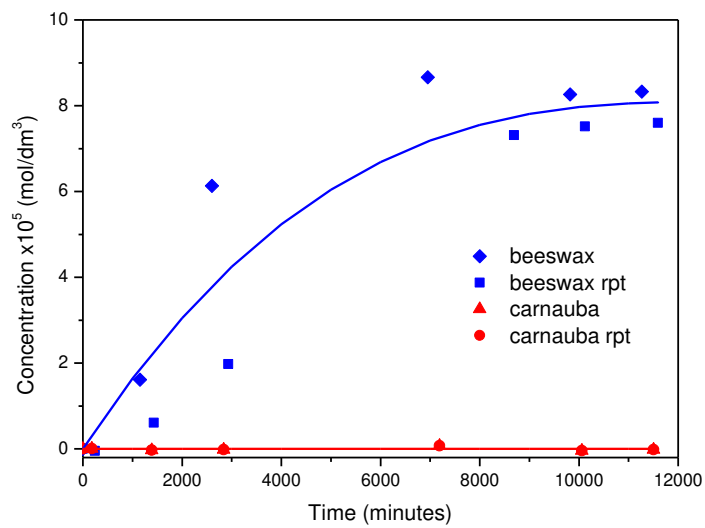


Figure 2d

Figure 2 Concentration profiles for a) apparatus only (using normal concentration and 10% of normal concentration); b) blank (filter paper), single dip coated beeswax and double dip coated beeswax; c) for single and double dip coated carnauba wax; d) for spin coated beeswax and spin coated carnauba wax (The lines are guide for the eye)

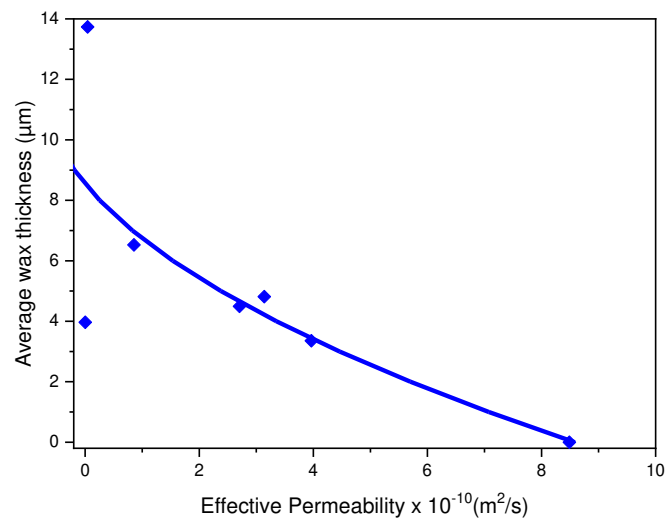


Figure 3 Thickness vs permeability for wax coated samples and uncoated filter paper (The line is a guide for the eye)

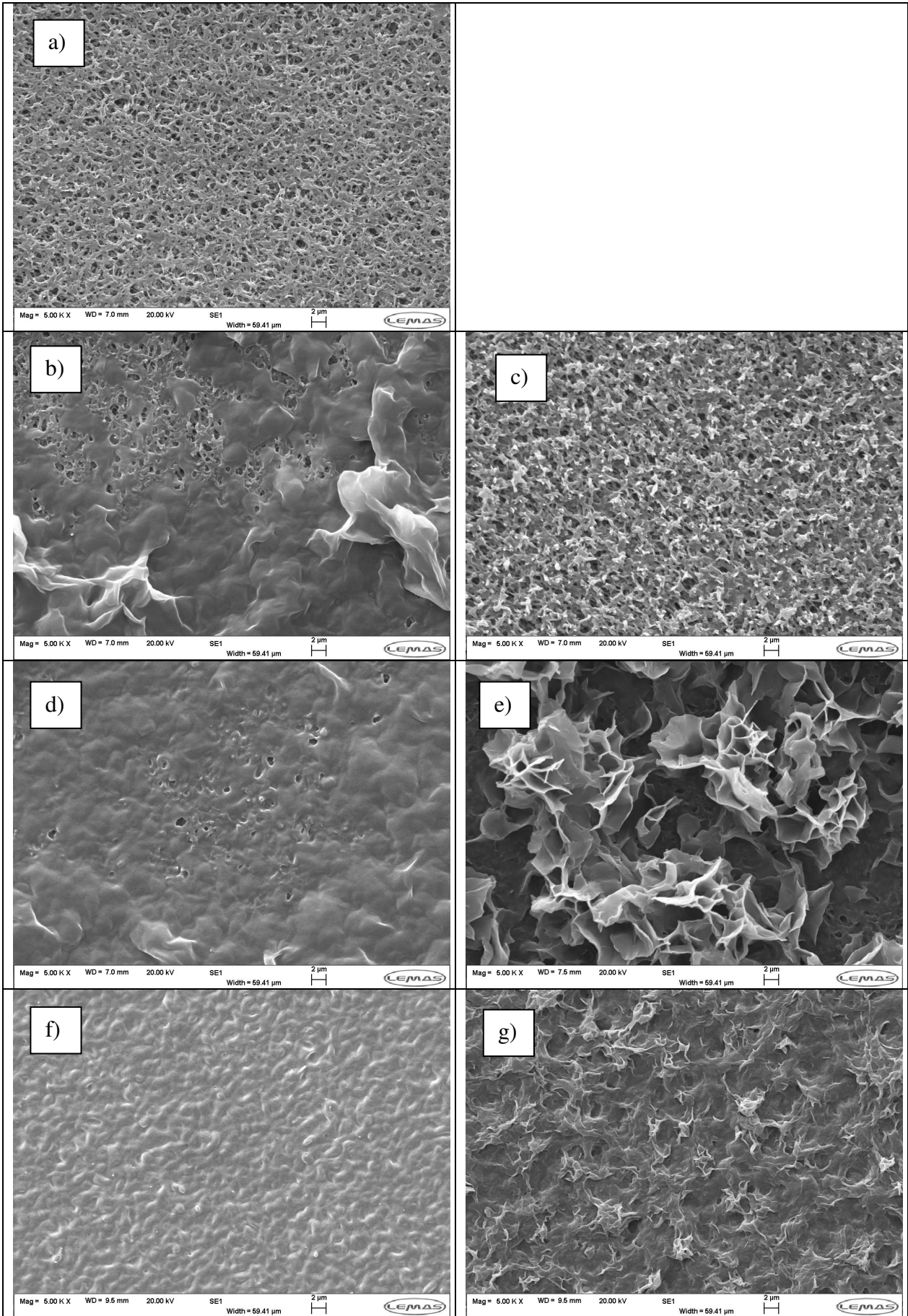


Figure 4 SEM images for a) untreated filter paper (0.1 μ m pore size), b) single dip beeswax, c) single dip carnauba wax, d) double dip beeswax, e) double dip carnauba wax, f) spin coated beeswax, g) spin coated carnauba wax (all same magnifications) (A larger range of magnifications is shown in Supplementary Information Figures S2-S5)

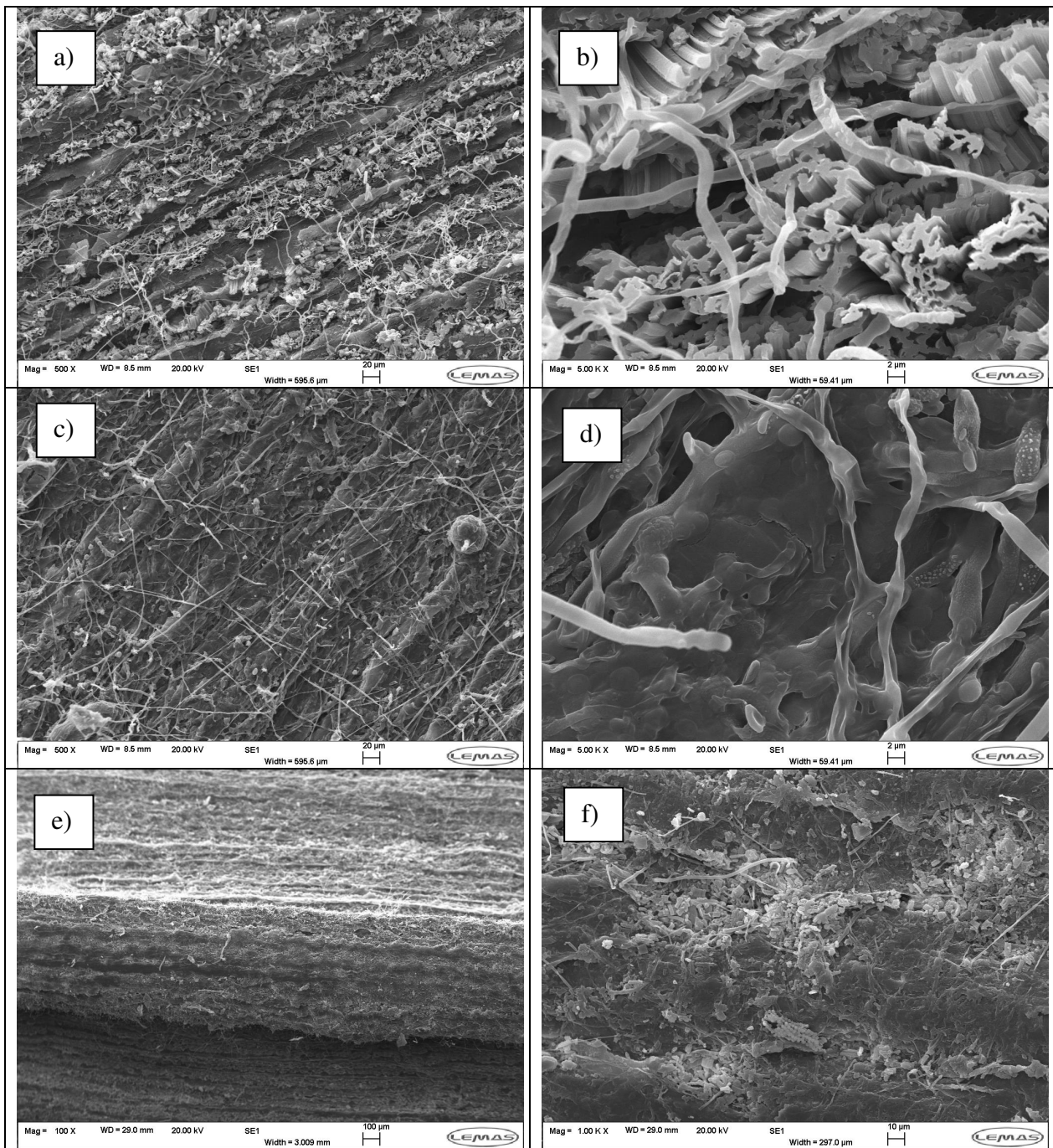


Figure 5 SEM images of leaf from *Copernicia prunifera*: a) and b) underneath whole leaf (same location different magnifications); c) and d) top whole leaf (same location different magnifications); e) and f) of ridge (underneath whole leaf) (same location different magnifications) (A larger range of magnifications is shown in Supplementary Information Figures S6-S7)

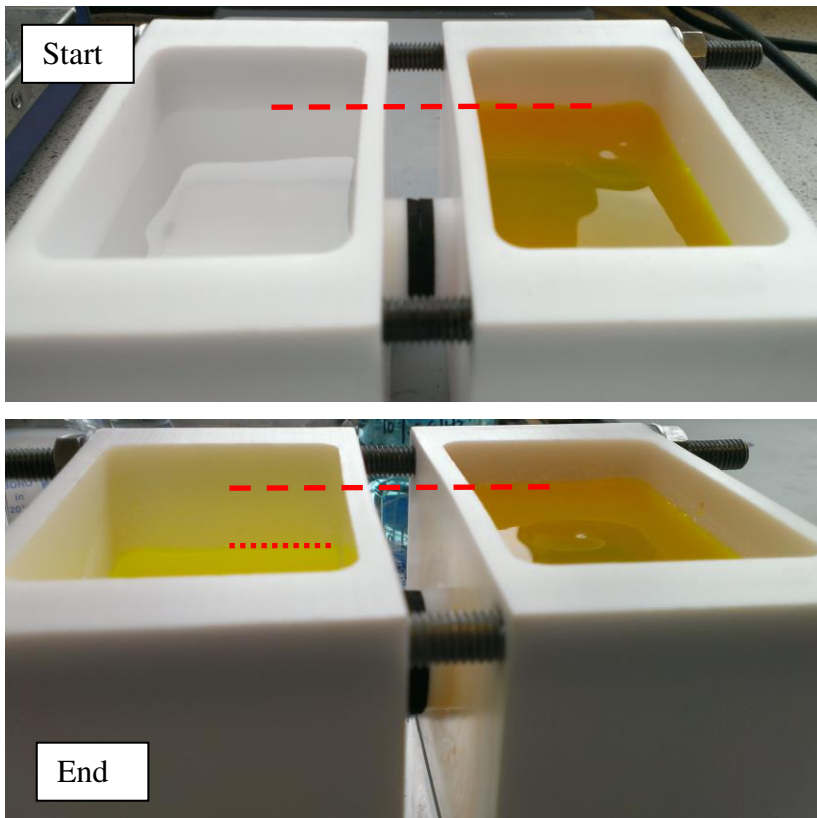


Figure 6 showing diffusion apparatus at the start (equal height levels) and end (unequal height levels) of a diffusion experiment showing levels in the two cells (left = “water”, right = “fluorescein solution”)